Recruitment of Regulatory T Cells with rCCL17 Promotes M2 Microglia/Macrophage Polarization Through TGFβ/TGFβR/Smad2/3 Pathway in a Mouse Model of Intracerebral Hemorrhage

Shuixiang Deng
Huashan Hospital Fudan University https://orcid.org/0000-0001-5460-7279
Peng Jin
The First Affiliated Hospital of USTC: Anhui Provincial Hospital
Shengpeng Liu
Shenzhen People's Hospital
Lei Huang
Loma Linda University School of Medicine
Prativa Sherchan
Loma Linda University School of Medicine
Yuhui Cui
Loma Linda University School of Medicine
John H. Zhang
Loma Linda University School of Medicine
Ye Gong
Huashan Hospital Fudan University
Jiping Tang (jtang@llu.edu)
Loma Linda University https://orcid.org/0000-0002-2392-9280

Research

Keywords: rCCL17, Regulatory T cells, Microglia/macrophage polarization, Inflammation, Intracerebral hemorrhage, mouse.

Posted Date: November 2nd, 2021

DOI: https://doi.org/10.21203/rs.3.rs-994135/v1

Abstract

Background

Intracerebral hemorrhage (ICH) is a devastating neurological disease with high mortality and morbidity. The microglia activation and peripheral inflammatory cells infiltration play an important role in the ICH prognosis. Previous studies have demonstrated that regulatory T cells (Tregs) ameliorated neuroinflammation following experimental ICH. However, the specific molecular mechanism underlying such effects of Tregs remains unclear. In the present study, our aims were to examine the effect of Tregs recruitment induced by recombinant CC chemokine ligand 17(rCCL17) in an intrastriatal autologous blood mouse model of ICH and to determine whether the TGF-β/TGF-βR/Smad2/3 pathway was involved in Tregs promoted M2 microglia/macrophage polarization.

Methods

A total of 404 adult CD1 mice (male, eight-week-old) were subject to sham surgery or autologous blood injection of ICH. A CD25-specific mouse antibody or isotype control mAb was injected intraperitoneally 48h prior to ICH induction to deplete Tregs. Recombinant CCL17 (rCCL17), a C-C chemokine receptor 4 (CCR4), was delivered intranasally at 1 h post-ICH. SB431542, a specific inhibitor of TGF-β was administered intraperitoneally 1 h before ICH induction. Post-ICH assessments included neuro-behavior evaluation, brain edema, hematoma volume, hemoglobin content, western blotting, double immunofluorescence staining and immunohistochemistry.

Results

Endogenous brain expressions of CCL17 and Tregs marker Foxp3 as well as the number of Tregs in the perihematomal region were increased following ICH. The Tregs deletion by a CD25 antibody aggravated short-term neurological deficits and brain edema, increased the level of inflammatory cytokines and peripheral inflammatory cells infiltration, exacerbated hematoma expansion and increased M1phenotypes of microglia/macrophage in ICH mice. The rCCL17 treatment increased the number of Tregs in the brain, reduced hematoma expansion and brain edema, promoted microglia/macrophage polarization toward M2 phenotypes. Moreover, the expressions of brain TGF-β/phosphorylated-Smad2/3 were increased. The neuroprotective effects of rCCL17 were abolished by co-administration of the selective TGF-β inhibitor SB431542.

Conclusions

Our study demonstrated rCCL17 recruited of Tregs to brain in the autologous blood injection model of ICH. Tregs promoted microglia/macrophages polarization toward M2 phenotype and alleviation early

brain injury, at least in part, through the TGFβ/TGFβR/Smad2/3 signaling pathway in ICH mice. Thus, rCCL17-mediated Tregs recruitment may provide a promising therapeutic strategy to reduce early brain injury after ICH.

Background

Spontaneous intracerebral hemorrhage (ICH) is a devastating cerebrovascular disease with high mortality and morbidity [1–3]. Accounting for 10–15% of stroke, the incidence of ICH shows a trend of increase with the growing elderly population in the worldwide [4–6]. Although there are many management options for ICH currently, there are no effective therapies to improve the prognosis of ICH patients. Microglia, the brain resident macrophage, has been proved to have a dual role following ICH. While M1 (classically) phenotype of microglia is pro-inflammatory, the M2 (alternatively) phenotype helps tissues repair through phagocytosis [7,8]. The M1 polarization microglia secretion of pro-inflammatory cytokines and hematoma-induced secondary neuroinflammation are considered as the critical factors participated in the pathogenesis of early brain injury after ICH [9,10]. Therefore, new treatments that facilitate M2 microglia polarization and inflammation suppression remain the interest of research in the setting of ICH.

Fork head box P3-expressing (Foxp3) regulatory T cells (Tregs), belonging to the family of CD4+T cells, play a critical role in regulating immune homeostasis by suppressing the immune system activation and inflammation [11]. Previous studies have demonstrated the neuroprotective role of Tregs in traumatic brain injury and cerebral ischemia [12–14]. In an animal model of ICH, Zhou and his colleagues showed that Tregs ameliorated neuroinflammation and promoted M2 microglia phenotypic transformation following ICH [15]. Therefore, Tregs becomes a promising therapeutic candidate for ICH specifically through its capability to suppress inflammatory cell infiltration and execute comprehensive therapeutic missions after migrating to peri-hematoma brain tissue [16,17].

ExogenousTregs infusion approach requires a long preparation time due to the complex extraction procedures in vitro and the number of Tregs extracted is limited. In addition, it is usually relied on local cell proximity or even directly cell-cell interactions for Tregs to perform its immune-suppressive function. Thus, it would be ideal to upregulate the endogenous Tregs migration and activation. C-C chemokine ligand 17 (CCL17), binding to its cognate CC chemokine receptor 4 (CCR4), play a critical role in orchestrating Tregs migration in vivo [18]. However, little is known about the effect of recombinant CCL17 (rCCL17) on the recruitment of Tregs after ICH. The aim of this study was to evaluate the rCCL17-mediated Tregs recruitment and its protective effects in mouse model of ICH. We further determined that the Tregs promoted M2 microglia/macrophage polarization via TGFβ/TGFβR/Smad2/3 pathway in ICH mice.

Materials And Methods

Animals and ICH Model

Adult male CD1 (8-week-old, 30-40 g, Charles River Laboratory, Wilmington, MA,USA) were used. Mice were housed in a room light of a 12-hour light/dark cycle and the temperature and humidity was controlled. All mice were free to access to water and food. ICH model was performed by striatal autologous blood injection as previously described [18].

Experimental Design

The following five separate experiments were performed.

Mice were randomized to experimental groups using a unique code linking to software-generated random numbers with 18.0 SPSS version. Investigators who conducted ICH surgeries and neurobehavioral tests were blinded to treatment assignments until the completion of data analysis.

Experiment 1

To examine the endogenous expressions of CCL17, Tregs marker Foxp3 and transforming growth factor-beta (TGF-β) after ICH, a total of 42 mice were randomly divided into 7 groups (n=6/group): sham, ICH-6h, ICH-12h, ICH-24h, ICH-72h,ICH-5d and ICH-7d for western blot. Additional 8 mice were used for immunofluorescence (IF) staining to localize Foxp3 in sham, ICH-24 h, ICH-72 h and ICH-7 d groups (n=2/group).

Experiment 2

To study the neuroprotective effect of endogenous Tregs following ICH, CD25-specific mAb was used to deplete Tregs at 48 h before ICH induction. Isotype control antibodies were used as control. This experiment was divided into two parts. The first part was to determine the efficacy of CD25-specific mAb on Tregs depletion after ICH. A total of 40 mice were randomly divided into 4 groups (n=10/group): sham + isotype control, sham + CD25-specific mAb, ICH + isotype control, ICH + CD25-specific mAb. Immunofluorescence (IF) staining and western blot were performed at 72 h post-ICH. The second part was to explore the protective effects of Tregs against ICH. 136 mice were randomly divided into the same 4 groups (n=34/group): sham + isotype control, sham + CD25-specific mAb, ICH + isotype control, ICH + CD25-specific mAb. Short-term neurobehavioral assessment (Corner Turn, Modified Garcia and Forelimb Placement Tests), hematoma volume and hemoglobin content were evaluated at 24 h, 72 h and 7 d following ICH. Brain water content was evaluated at 72 h post-ICH and immumohistochemical staining and western blot were used for assessing neuroinflammation at 72 h post-ICH.

Experiment 3

To determine the neuroprotective effect of rCCL17 was via upregulating peripheral Tregs recruitment into brain following ICH. This experiment was divided into two parts. The first part was to determine the effect of rCCL17 on peripheral Tregs recruitment after ICH. A total of 16 mice were randomly divided into 4 groups (n=4/group): sham + vehicle, sham + rCCL17 (30 μg/kg), ICH + vehicle, ICH + rCCL17 (30 μg/kg). Immumohistochemical and immunofluorescence staining were performed at 72 h post-ICH to evaluate

the number of Tregs in ipsilateral brain hemisphere. Then, the second part was to explore whether neuroprotective effects of rCCL17 were depended on Tregs recruitment following ICH. A total of 72 mice were randomly divided into 4 groups (n=18/group): sham + isotype control, sham + CD25-specific mAb, ICH + isotype control, ICH + CD25-specific mAb. Neurobehavioral function, hematoma volume and hemoglobin content, brain water content, western blot were performed at 72 h post-ICH.

Experiment 4

To investigate the effects of Tregs recruitments on microglia/macrophage polarization after ICH, a total of 40 mice were randomized to 4 groups ((n=10/group)): ICH + isotype control, ICH + CD25-specific mAb, ICH + isotype control + rCCL17 (30 μg/kg), ICH + CD25-specific mAb + rCCL17 (30 μg/kg). Western blot and immunofluorescence staining were conducted to evaluate the microglia/macrophage polarization at 72 h following ICH.

Experiment 5

To investigate the mechanism of TGFβ/TGFβ1R/Smad2/3 pathway underlying the neuroprotective effects of Tregs in brain after ICH, a total of 50 mice were divided into 5 groups (n=10/group): sham, ICH + vehicle, ICH + rCCL17 (30 μg/kg), ICH + rCCL17 (30 μg/kg) + DMSO, ICH + rCCL17 (30 μg/kg) + SB431542. Western blot and immunofluorescence staining were performed at 72 h following ICH.

Drug Administration

At 1 h after ICH, rCCL17 (14013, LSBio, WA) at dose of 30 ug/kg was delivered intranasally (i.n.) as previously reported [18]. SB431542 (ab120163, Abcam, USA) (1 μM solution, 100 μl/animal) was administrated intraperitoneally (i.p.) 1 h before the ICH induction. A total of 300mg of CD25-specific mAb (10200, biolegend, CA) or isotype control antiboy ((401602, biolegend, CA) was administered intraventricularly (i.c.v) route 48 h before the ICH induction as previously reported [19].

Short-term Neurobehavioral Assessment

The modified Garcia test with a twenty-one scoring system, corner turn test and the forelimb placement test (a positive percentage of total of 10 trials) were evaluated at 24 h, 72 h and 7 d after ICH as previously published from our lab[20].

Brain Water Content Measurement

Brain water content was measured using the wet/dry method as previously reported [21]. In brief, the brains were divided into 5 parts: left basal ganglia, left cortex, right basal ganglia, right cortex and cerebellum. Each part was measured immediately as the wet weight and then measured again as the dry weight after 48 h incubation in 100°C oven. Brain water content was calculated using the following formula: (Wet Weight−Dry Weight)/Wet Weight*100% to calculate.

Measurement of Hematoma Volume and Hemoglobin Content

Spectrophotometric measurement of hematoma volume and Drabkin's reagent measurement of hemoglobin content were accessed at 24 h, 72 h and 7 d following the ICH induction as previously reported [19].

Western Blot

Western blot was performed as previously described [22]. In brief, mice were perfused with cold PBS by transcardially. The right ipsilateral hemispheres were immediately harvested and mixed with RIPA. Supernatants were collected after centrifuged at 14 000g for 30 minutes (4°C). A total of 4 μL protein samples were loaded onto the SDS-PAGE gel and transferred to a nitrocellulose membrane. The membranes were incubated with the primary antibodies against CCL17 (1:1000, ab182793, Abcam, USA), Foxp3 (1:1000, ab182793, Abcam, USA), TGF-β (1:1000, GTX103322, Gene Tex), IL-1β (1:1000, ab9722, Abcam, USA), TNF-α (1:1000, ab6671, Abcam, USA), CD68 (1:1000, sc-97778, Santa Cruz Biotechnology, USA), CD206 (1:1000, sc-70585, Santa Cruz Biotechnology, USA), Smad2/3 (1:1000, Santa Cruz Biotechnology, USA) overnight at 4°C. The membranes were incubated with secondary antibodies at the second day and β-actin was used as a control. The relative density of the bands was analyzed with Image J software.

Immunofluorescence staining

Immunofluorescence staining was conducted at 72 h after ICH as previously described [23]. Briefly, formalin fixed, frozen, brain samples were cut into 10 mm-thick sections. The sections were incubated with primary antibodies against Foxp3 (1:100, ab182793, Abcam, USA), CD68 (1:100, sc-97778, Santa Cruz Biotechnology, USA), CD206 (1:100, sc-70585, Santa Cruz Biotechnology, USA) over-night at 4°C. On the second day, the slices were incubated with appropriate secondary antibodies for 2 h at room temperature. After adding DAPI (4', 6-diamidino-2-phe-nylindole) the slides were cover slipped. The staining were observed and photographed using a DMi8 fluorescent microscope under a 400 × fold field.

Immunohistochemistry

Immunohistochemistry was performed as described previously [24].Briefly, the mice were euthanized at 72 h after ICH. Brain samples were fixed in formalin, gradient dehydrated in 30% sucrose, and embed in OTC. The sliced brain samples were rinsed and blocked with 5% donkey serum. Myeloperoxidase (MPO), CD3, and Foxp3 immunochemistry staining was conducted using MPO antibody (1:200, ab208670, Abcam, USA), CD3 (1:200, sc-78588, Santa Cruz Biotechnology, USA), and Foxp3 antibody (1:100, ab182793, Abcam, USA). The staining was observed and photographed using a DMi8 fluorescent microscope under a 400 × fold field.

Statistical Analysis

Results were expressed as mean ± SD. The statistical analyses were performed using GraphPad Prism 7 (La Jolla, CA, USA). One-way ANOVA following by T-ukey post hoc test was used to evaluate quantitative western blot, brain water content and cell counting data. Two-way ANOVA following by T-ukey post hoc test was used to compare behavior data, hematoma volume and hemoglobin content. Statistical significance was considered as if P values were < 0.05.

Results

Animal mortality rate

A total number of 404 were used in this study, of which 254 underwent ICH and 150 were shams. Three mice died due to deep anesthesia prior to ICH-induction and there mice died during the procedure of i.c.v injection of the CD25 antibody. No mice died in sham group. The ICH-surgery mortality was 2.36%.

Temporal patterns and Tregs accumulate in brain after ICH

Western blot results showed that the expressions of CCL17, Tregs marker Foxp3 and TGF-β started to increase at 12 h and peaked at 5-7 days post-ICH (Figure 1A-D). Immunofluorescence staining consistently revealed that $Foxp3^+$ Tregs within ipsilateral hemisphere were increased at 1 d and peaked at 7 d after ICH (Figure 1E and 1F).

Tregs depletion aggravated the early brain injury after ICH

The i.c.v injection of CD25 antibody at 48 h before ICH significantly decreased the endogenous expressions of Foxp3 and the number of $Foxp3^+$ cells in sham and ICH mice, suggesting the Tregs depletion efficacy of CD25 antibody in the present study (Fig. 2A– E).Compared with the isotype IgG pre-treated ICH control group, the Tregs depletion by CD25 antibody pre-treatment significantly exacerbated the neurobehavioral deficits including the modified Garcia score, corner turn test and the forelimb placement test at 72 h and 7 d after ICH (Fig. 3A). Tregs depletion leaded to an expansion in hematoma volume and an increase in hemoglobin levels at 72 h and 7 d after ICH (Figure 3B-D). Tregs depletion also resulted in an increase in water content (Figure 3E), and the greater expression of proinflammatory IL-1β and TNF-a, but the expression of TGF-β remained low (Figure 4A-D) at 72 h after ICH. Immuno-histochemical staining showed Tregs depletion significantly increased MPO^+ and $CD3^+$ cells in the peri-hematoma region compared to controls at 72 h after ICH (Figure 4E-F).

Tregs recruitment by rCCL17 alleviated early brain injury after ICH

Previous studies have indicated that CCL17/CCR4 axis activation can recruit Tregs in vivo. To clarify the effect of rCCL17 in Tregs chemotaxis to brain after ICH, rCCL17 was administrated i.n. 1 h after ICH. At 72 h after ICH, immune-histochemical and IF staining results showed a significant increased Tregs in the peri-hematoma region of brain in rCCL17-ICH group compared with the isotype-ICH control group (Figure 5A-D).

In addition, compared with the isotype-ICH control group at 72 h after ICH, rCCL17 administration alleviated neurobehavioral deficits (Fig. 5E), reduced brain edema (Figure 5F). Moreover, rCCL17 administration significantly attenuated hematoma volume and hemoglobin levels in ICH mice compared to that in the isotype-ICH control group (Figure 6A-C), and decreased the expression of IL-1β and TNF-a, increased the expression of TGF-β (Figure 6D-G).

Tregs promoted microglial/macrophages polarization and shifted toward M2 phenotype after ICH

Double immunofluorescence staining was used to access the Tregs-induced M2 microglia/macrophages polarization. The results showed that Tregs depletion in by CD25 antibody significantly increased $CD68^+$ M1 microglial/macrophages but decreased $CD206^+$ M2 microglial/macrophages in ICH mice when compared with isotype-ICH control group (Fig. 7A-D). The upregulated recruitment of Tregs by rCCL17 administration resulted in increases in $CD206^+$ M2 microglial/macrophages but decreased $CD68^+$ M1 microglial/macrophages in ICH + isotype control + rCCL17 group compared with the ICH + isotype control group, ICH + CD25 antibody group and ICH + CD25 antibody + rCCL17 group(Fig. 7A-D).

Similarly, western blot analysis showed that Tregs depletion significantly increased CD68 protein levels but decreased CD206 expressions in the ipsilateral hemisphere of ICH + CD25 antibody group compared with the ICH + isotype control group (Fig. 7E-G). Intransal rCCL17 treatment resulted in increases in CD206 expressions but decreased CD68 expression in ICH + isotype control + rCCL17 group compared with the ICH + isotype control group, ICH + CD25 antibody group and ICH + CD25 antibody + rCCL17 group (Fig. 7E-G).

TGFβ/TGFβR/Smad2/3 axis participated in Tregs-induced M2 microglial/macrophages polarization in brain after ICH

Double immunofluorescence staining results showed that rCCL17 treatment resulted in increases in $CD206^+$ M2 microglial/macrophages while decreased $CD68^+$ M1 microglial/macrophages in ICH + rCCL17 group compared with the ICH + vehicle group (Fig. 8A-D). Pretreatment with the TGF-β inhibitor, SB431542, significantly abolished the effect of rCCL17 resulting in the increased $CD68^+$ M1 microglial/macrophages but decreased in $CD206^+$ M2 microglial/macrophages compared with the ICH + rCCL17 and ICH + rCCL17 +DMSO group (Fig. 8A-D).

Similarly, western blot analysis showed rCCL17 treatment resulted in increased expressions of TGF-β, p-Smad2/3 and CD206 but decreased CD68 expressions in ICH + rCCL17 group compared with the ICH + vehicle group (Fig. 8E-I). Pretreatment with the selective TGF-β inhibitor SB431542 significantly abolished the effect of rCCL17 resulting in a higher CD68 expression but lower expression of p-Smad2/3 and CD206 compared with the ICH + rCCL17 and ICH + rCCL17 +DMSO group (Fig. 8E-I).

Discussion

In the present study, we first investigated the neuroprotective effects of rCCL17-mediated Tregs recruitment into brain after ICH and mechanism of Tregs-induced M2 microglia/macrophage polarization in a mouse model of ICH. The results showed that 1) the expression levels of endogenous CCL17, Tregs marker Foxp3 and TGF-β were significantly increased at 5 d and 7 d after ICH compared with the sham group. The number of Tregs in the peri-hematoma region was increased and peaked at days 7 after ICH; 2) Tregs depletion by the CD25 antibody aggravated the early brain injury and deteriorated neurological deficits after ICH, while rCCL17-medicated Tregs recruitment into brain alleviated early brain injury after ICH; 3) Recruitment of Tregs promoted microglial/macrophages polarization and shifted toward M2 phenotype after ICH, at least in part, through TGFβ/TGFβR/Smad2/3 signaling pathway.

Tregs, a Foxp3-expressing subset of $CD4^+$ T cells, play a critically role in preserving immune homeostasis under normal physiological conditions and are characterized as protective cells in limiting inflammation-related damage in several inflammatory conditions including central nervous system (CNS)[25,26] In cancer cells, Tregs infiltration can help the cancer cells escape from immunological cells elimination which was correlated with worse prognosis in a variety of cancer types [25,27,28]. In CNS, Tregs modulate immune tolerance and provide anti-inflammatory effects in animal model of ischemic stroke, traumatic brain injury and ICH [13–15,29]. However, little is known about the regulatory mechanism underlying the brain recruitment of Tregs and M2 microglia/macrophage polarization effects of Tregs against ICH.

Inflammatory processes characterized by the infiltration of peripheral inflammatory cells and release of proinflammatory cytokines play an important role in the pathophysiology of ICH [17]. Due to a very low number of Tregs in the brain under normal conditions, the characteristics and functions of brain intrinsic Tregs in modulating immune balance is largely unexplored after ICH. In the present study, we found that there was abundant accumulation of Tregs in the hemorrhagic hemisphere and Tregs depletion by CD25 antibodies aggravated early brain damage and exacerbated neurobehavioral deficits at 72 h after ICH. The results are consistent with previous report by others that Tregs were neuroprotective following ICH [15,30]. In Tregs depleted mice, we further found an increased infiltration of proinflammatory MPO^+ and $CD3^+$ T cells into the ipsilateral brain hemisphere and greater the M1 microglial/macrophages at 72h after ICH, which indicated Tregs recruitment as a endogenous protective mechanism of body in response to ICH.

CCL17, predominantly expression in macrophage lineage populations and neurons [31,32], was primarily involved in a broader biology of attraction of $CD4^+$ Tregs via binding to its receptor, CCR4, in multiple sclerosis [33], endotoxin shock and inflammatory pain [34]. In the current study, we found rCCL17-mediated Tregs recruitment into peri-hematoma regions alleviated the early brain injury by promoting the M2 polarization of microglial/macrophages after ICH. In the early stages of ICH, microglia is the first innate immune response cell among non-neuronal cells [7,35].

Microglia activated and polarized into classic M1-like (proinflammatory) phenotype to produce toxic chemicals that further exacerbate the blood brain barrier dysfunction and peripheral proinflammatory

cells infiltration. After 3–4 days after ICH, the shifting of M1-type microglia/macrophages into alternative M2-like (anti-inflammatory) phenotype promotes phagocytosis of red blood cells scavenges necrotic cells and facilitates neural repair [7,36]. Therefore, therapeutic approach promoting microglia/macrophages polarization toward M2 phenotypes would be effective in attenuating of brain injury after ICH. Previous studies demonstrated that Tregs proliferation induced by CD28 superagonistic monoclonal or infusion isolated Tregs prevented secondary brain damage and promoted M2 microglia/macrophages polarization after ICH [15,30,37]. CD28 superagonistic antibodies can cause activation and proliferation of Tregs regardless of signal received by T-cell receptor. However, its treatment efficiency was uncertain of using antibody injection to boost Tregs in vivo after ICH. Thus, rCCL17 appears to offer a feasible and efficient way to up-regulate peripheral Tregs migration into brain that promote M2 microglia/macrophages polarization after ICH in mice.

Furthermore, we further explored the interaction between Tregs and microglia. Our study showed that Tregs promoted microglial/macrophages shifted toward M2 phenotype via TGFβ/TGFβR axis after ICH. Early studies showed that TGF-β originating from Tregs can activate M2 microglia and suppress inflammation [38,39] through Smad2/3 signaling [40–42].

Consistently, we found that blockade of TGF-β receptor (TGF-βR) by SB431542 reversed the effects of rCCL17 on M2 microglial/macrophages polarization. It is likely that rCCL17-recruited Tregs released TGF-β in the brain. TGF-β binds to microglia TGF-β receptor and activated the downstream Smad2/3 signal pathway that further promote microglial/macrophages polarization into M2 phen0-type, thus leading to hematoma clearance, less neuroinflammation and improved neurobehavioral deficit in ICH.

There are several limitations in the current study. First, this study mainly focused on the neuroprotective effect of rCCL17-mediated Tregs recruitment against early brain injury after ICH. Additional long-term study is needed for further validate such protection. Second, anti-CD25 mAb depletes all $CD25^+$ cells including activated T and B cells. We could not exclude the depletion effects of B cells and other T cells on the outcome after ICH. Further study is necessary to use transgenic mice with a diphtheria toxin receptor (DTR) to induce specific Tregs depletion after ICH. At last, our data demonstrated TGFβ/TGFβR/Smad2/3 signaling in M2 microglia/macrophages polarization modulated by Tregs. However, other signaling pathways such as IL-10 and JNK may also be involved as potential underlying mechanisms.

Conclusions

Our study demonstrated rCCL17-mediated Tregs recruitment into brain attenuated the early brain injury and promoted M2 microglia/macrophages polarization, at least in part, through the TGFβ/TGFβR/Smad2/3 signaling pathway in mouse model of ICH. Thus, therapeutic strategy that up-regulates Tregs recruitment to injured brain may provide a promising approach in treatment of ICH patients.

Abbreviations

ICH, intracerebral hemorrhage, CCL17, C-C chemokine ligand17, rCCL17, Recombination C-C chemokine ligand17, CCR4, C-C Chemokine Receptor 4, IF, Immunofluorescence, BWC, brain water content, DMSO, Dimethyl sulfoxide, i.n., intranasally, i.c.v, intracerebroventricularly. Foxp3, Fork head box P3-expressing, Tregs, regulatory T cells, TGF-β, transforming growth factor-beta, i.p., intraperitoneally, MPO, Myeloperoxidase, CNS, central nervous system, TGF-βR, TGF-β receptor, DTR, diphtheria toxin receptor.

Declarations

Acknowledgements

Not applicable.

Ethics approval and consent to participate

All experiment protocols were conducted in the light of the guidelines of care and use of laboratory animals of the National Institutes of Health and approved by Animal Care and Use Committee of Loma Linda University.

Availability of data and materials

All original experimental data supporting this experiment may be provided by the corresponding author upon reasonable request.

Funding

This study is supported partially by grants from National Institutes of Health (NS082184 to John Zhang, NS101284 to Jiping Tang) and by grants from the Science and Technology Commission of Shanghai Municipal (21ZR1410700 to S.D.).

Authors' contributions

SXD and PS participated in the experimental design. SXD, PJ and SPL conducted the experiments. YHC analyzed the data and HL revised the paper. JHZ, YG and JPT participated in the experimental design and manuscript preparation. All authors read and approved the final manuscript.

Consent for publication

Not applicable.

Competing interests

The authors declare that they have no competing interests.

References

1. Withers SE, Parry-Jones AR, Allan SM, Kasher PR. A Multi-Model Pipeline for Translational Intracerebral Haemorrhage Research. Translational stroke research 2020,11:1229-42.
2. Zhang S, Hu ZW, Luo HY, et al. AAV/BBB-Mediated Gene Transfer of CHIP Attenuates Brain Injury Following Experimental Intracerebral Hemorrhage. Translational stroke research 2020,11:296-309.
3. Zhang Z, Cho S, Rehni AK, Quero HN, Dave KR, Zhao W. Automated Assessment of Hematoma Volume of Rodents Subjected to Experimental Intracerebral Hemorrhagic Stroke by Bayes Segmentation Approach. Translational stroke research 2020,11:789-98.
4. Shi SX, Li YJ, Shi K, Wood K, Ducruet AF, Liu Q. IL (Interleukin)-15 Bridges Astrocyte-Microglia Crosstalk and Exacerbates Brain Injury Following Intracerebral Hemorrhage. Stroke 2020,51:967-74.
5. Liddle LJ, Ralhan S, Ward DL, Colbourne F. Translational Intracerebral Hemorrhage Research: Has Current Neuroprotection Research ARRIVEd at a Standard for Experimental Design and Reporting? Translational stroke research 2020,11:1203-13.
6. Tao C, Keep RF, Xi G, Hua Y. CD47 Blocking Antibody Accelerates Hematoma Clearance After Intracerebral Hemorrhage in Aged Rats. Translational stroke research 2020,11:541-51.
7. Lan X, Han X, Li Q, Yang QW, Wang J. Modulators of microglial activation and polarization after intracerebral haemorrhage. Nature reviews Neurology 2017,13:420-33.
8. Michell-Robinson MA, Touil H, Healy LM, et al. Roles of microglia in brain development, tissue maintenance and repair. Brain : a journal of neurology 2015,138:1138-59.
9. Chang CF, Massey J, Osherov A, Angenendt da Costa LH, Sansing LH. Bexarotene Enhances Macrophage Erythrophagocytosis and Hematoma Clearance in Experimental Intracerebral Hemorrhage. Stroke 2020,51:612-8.
10. Xu J, Chen Z, Yu F, et al. IL-4/STAT6 signaling facilitates innate hematoma resolution and neurological recovery after hemorrhagic stroke in mice. Proceedings of the National Academy of Sciences of the United States of America 2020.
11. Esensten JH, Muller YD, Bluestone JA, Tang Q. Regulatory T-cell therapy for autoimmune and autoinflammatory diseases: The next frontier. The Journal of allergy and clinical immunology 2018,142:1710-8.
12. Liesz A, Kleinschnitz C. Regulatory T Cells in Post-stroke Immune Homeostasis. Translational stroke research 2016,7:313-21.
13. Ito M, Komai K, Mise-Omata S, et al. Brain regulatory T cells suppress astrogliosis and potentiate neurological recovery. Nature 2019,565:246-50.
14. Krämer TJ, Hack N, Brühl TJ, et al. Depletion of regulatory T cells increases T cell brain infiltration, reactive astrogliosis, and interferon-γ gene expression in acute experimental traumatic brain injury. Journal of neuroinflammation 2019,16:163.
15. Zhou K, Zhong Q, Wang YC, et al. Regulatory T cells ameliorate intracerebral hemorrhage-induced inflammatory injury by modulating microglia/macrophage polarization through the IL-

10/GSK3β/PTEN axis. Journal of cerebral blood flow and metabolism : official journal of the International Society of Cerebral Blood Flow and Metabolism 2017,37:967-79.

16. Neal EG, Acosta SA, Kaneko Y, Ji X, Borlongan CV. Regulatory T-cells within bone marrow-derived stem cells actively confer immunomodulatory and neuroprotective effects against stroke. Journal of cerebral blood flow and metabolism : official journal of the International Society of Cerebral Blood Flow and Metabolism 2019,39:1750-8.
17. Zhao W, Wu C, Stone C, Ding Y, Ji X. Treatment of intracerebral hemorrhage: Current approaches and future directions. Journal of the neurological sciences 2020,416:117020.
18. Ruland C, Renken H, Kuzmanov I, et al. Chemokine CCL17 is expressed by dendritic cells in the CNS during experimental autoimmune encephalomyelitis and promotes pathogenesis of disease. Brain, behavior, and immunity 2017,66:382-93.
19. Deng S, Sherchan P, Jin P, et al. Recombinant CCL17 Enhances Hematoma Resolution and Activation of CCR4/ERK/Nrf2/CD163 Signaling Pathway After Intracerebral Hemorrhage in Mice. Neurotherapeutics : the journal of the American Society for Experimental NeuroTherapeutics 2020.
20. Yan J, Zuo G, Sherchan P, et al. CCR1 Activation Promotes Neuroinflammation Through CCR1/TPR1/ERK1/2 Signaling Pathway After Intracerebral Hemorrhage in Mice. Neurotherapeutics : the journal of the American Society for Experimental NeuroTherapeutics 2020.
21. Chen S, Peng J, Sherchan P, et al. TREM2 activation attenuates neuroinflammation and neuronal apoptosis via PI3K/Akt pathway after intracerebral hemorrhage in mice. Journal of neuroinflammation 2020,17:168.
22. Luo Y, Fang Y, Kang R, et al. Inhibition of EZH2 (Enhancer of Zeste Homolog 2) Attenuates Neuroinflammation via H3k27me3/SOCS3/TRAF6/NF-κB (Trimethylation of Histone 3 Lysine 27/Suppressor of Cytokine Signaling 3/Tumor Necrosis Factor Receptor Family 6/Nuclear Factor-κB) in a Rat Model of Subarachnoid Hemorrhage. Stroke 2020,51:3320-31.
23. Zhang T, Wu P, Budbazar E, et al. Mitophagy Reduces Oxidative Stress Via Keap1 (Kelch-Like Epichlorohydrin-Associated Protein 1)/Nrf2 (Nuclear Factor-E2-Related Factor 2)/PHB2 (Prohibitin 2) Pathway After Subarachnoid Hemorrhage in Rats. Stroke 2019,50:978-88.
24. Lee HT, Liu SP, Lin CH, et al. A Crucial Role of CXCL14 for Promoting Regulatory T Cells Activation in Stroke. Theranostics 2017,7:855-75.
25. Wing JB, Tanaka A, Sakaguchi S. Human FOXP3(+) Regulatory T Cell Heterogeneity and Function in Autoimmunity and Cancer. Immunity 2019,50:302-16.
26. van der Veeken J, Gonzalez AJ, Cho H, et al. Memory of Inflammation in Regulatory T Cells. Cell 2016,166:977-90.
27. Plitas G, Konopacki C, Wu K, et al. Regulatory T Cells Exhibit Distinct Features in Human Breast Cancer. Immunity 2016,45:1122-34.
28. Tanaka A, Sakaguchi S. Regulatory T cells in cancer immunotherapy. Cell research 2017,27:109-18.
29. Ito M, Komai K, Nakamura T, Srirat T, Yoshimura A. Tissue regulatory T cells and neural repair. International immunology 2019,31:361-9.

30. Mao LL, Yuan H, Wang WW, et al. Adoptive Regulatory T-cell Therapy Attenuates Perihematomal Inflammation in a Mouse Model of Experimental Intracerebral Hemorrhage. Cellular and molecular neurobiology 2017,37:919-29.
31. Scheu S, Ali S, Ruland C, Arolt V, Alferink J. The C-C Chemokines CCL17 and CCL22 and Their Receptor CCR4 in CNS Autoimmunity. International journal of molecular sciences 2017,18.
32. Fülle L, Offermann N, Hansen JN, et al. CCL17 exerts a neuroimmune modulatory function and is expressed in hippocampal neurons. Glia 2018,66:2246-61.
33. Yoshie O, Matsushima K. CCR4 and its ligands: from bench to bedside. International immunology 2015,27:11-20.
34. Lee KM, Jarnicki A, Achuthan A, et al. CCL17 in Inflammation and Pain. Journal of immunology (Baltimore, Md : 1950) 2020,205:213-22.
35. Rahman MS, Yang J, Luan Y, et al. Attenuation of Acute Intracerebral Hemorrhage-Induced Microglial Activation and Neuronal Death Mediated by the Blockade of Metabotropic Glutamate Receptor 5 In Vivo. Neurochemical research 2020,45:1230-43.
36. Yang P, Manaenko A, Xu F, et al. Role of PDGF-D and PDGFR-β in neuroinflammation in experimental ICH mice model. Experimental neurology 2016,283:157-64.
37. Yang Z, Yu A, Liu Y, et al. Regulatory T cells inhibit microglia activation and protect against inflammatory injury in intracerebral hemorrhage. International immunopharmacology 2014,22:522-5.
38. Taylor RA, Chang CF, Goods BA, et al. TGF-β1 modulates microglial phenotype and promotes recovery after intracerebral hemorrhage. The Journal of clinical investigation 2017,127:280-92.
39. Butovsky O, Jedrychowski MP, Moore CS, et al. Identification of a unique TGF-β-dependent molecular and functional signature in microglia. Nature neuroscience 2014,17:131-43.
40. Abutbul S, Shapiro J, Szaingurten-Solodkin I, et al. TGF-β signaling through SMAD2/3 induces the quiescent microglial phenotype within the CNS environment. Glia 2012,60:1160-71.
41. Neidert N, von Ehr A, Zöller T, Spittau B. Microglia-Specific Expression of Olfml3 Is Directly Regulated by Transforming Growth Factor β1-Induced Smad2 Signaling. Frontiers in immunology 2018,9:1728.
42. Yu Y, Li J, Zhou H, Xiong Y, Wen Y, Li H. Functional importance of the TGF-β1/Smad3 signaling pathway in oxygen-glucose-deprived (OGD) microglia and rats with cerebral ischemia. International journal of biological macromolecules 2018,116:537-44.

Figures

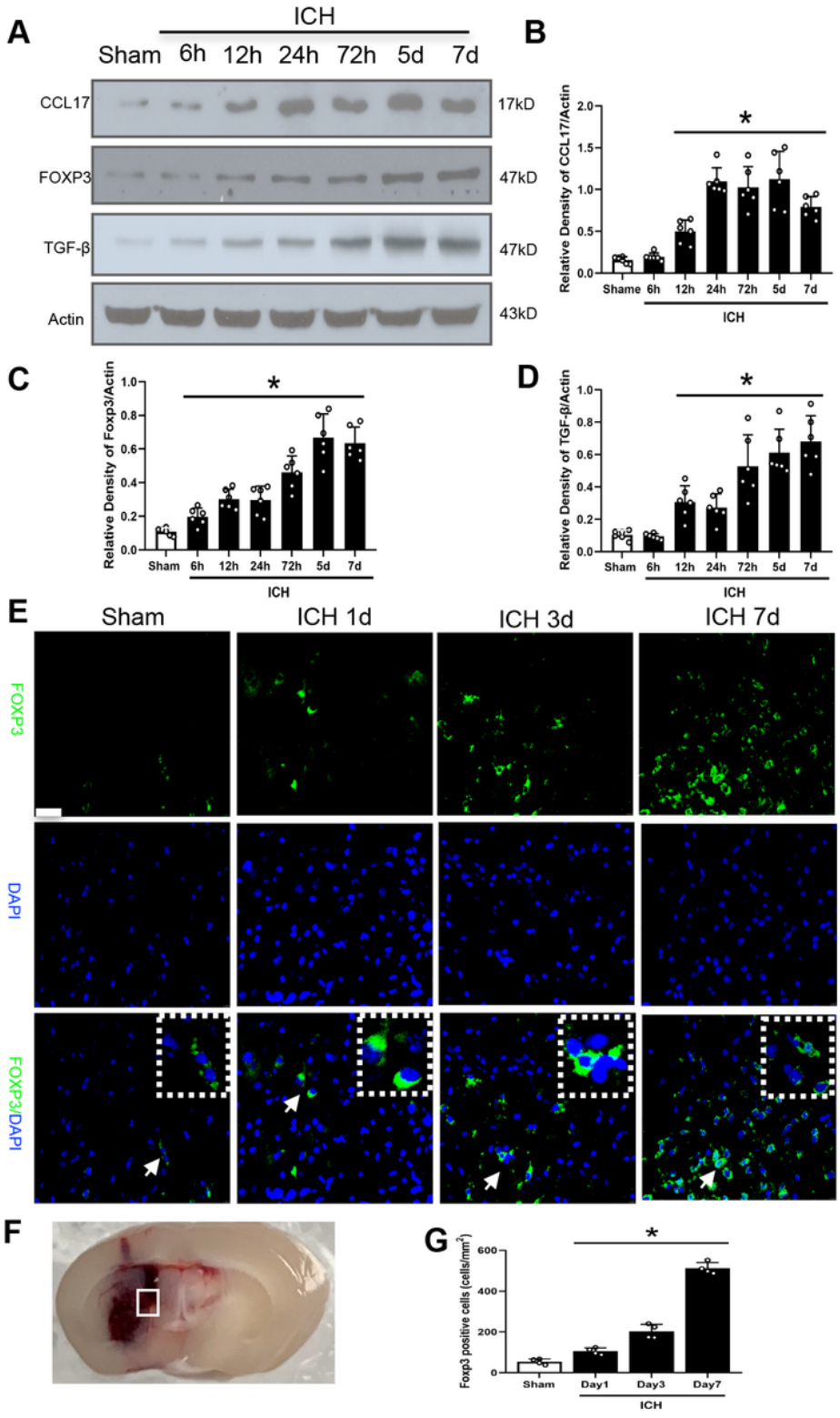

Figure 1

Expressions of CCL17 (C-C chemokine ligand17), Foxp3 (Fork head box P3-expressing), and TGF-β (Transforming growth factor-β) in ipsilateral brain hemisphere after intracerebral hemorrhage (ICH). A-D, Representative western blot images and quantitative analyses of CCL17, Foxp3 and TGF-β time course after ICH. n=6/group, * p<0.05 vs. sham, Mean ± SD, One-way ANOVA, Tukey test. E, Brain samples with schematic illustration showing the peri-hematomal region (small white box) from where the

microphotograph of immunofluorescence staining was taken. F, Representative microphotograph showed the localization of Foxp3-positive cells (green) in the perihematomal area at 1 d, 3 d and 7 d after ICH. Nuclei were stained with DAPI (blue), scale bar=50 μm, n=2/group, DAPI, 4',6-diamidino-2-phenylindole.

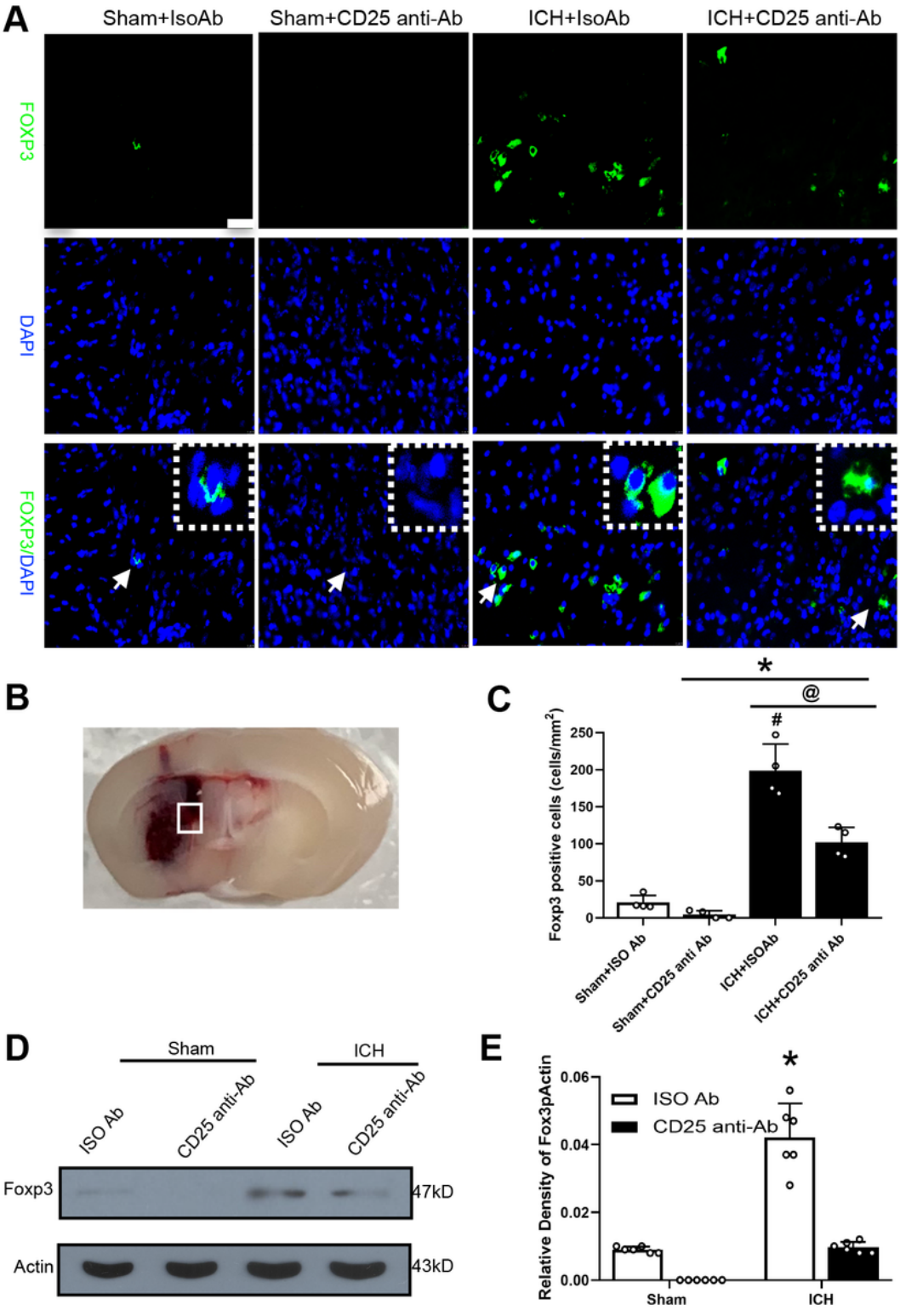

Figure 2

The depletion efficacy of the CD25 antibody on Tregs. A, Representative microphotograph of localization of Foxp3+ cells (green) in the peri-hematomal area at 72 h after ICH. Nuclei were stained with DAPI (blue),

scale bar=50 μm, n=2/group. B, Brain samples with schematic illustration showing the peri-hematomal region (small white box) from where the microphotograph of immunofluorescence staining was taken. C, Quantitative analysis of Foxp3-positive cells within the ipsilateral hemisphere at 72 h after ICH. n=4/group. D-E, Representative western blot bands and quantitative analyses of Foxp3 at 72 h after ICH. n=6/group, * p<0.05 vs. sham + isotype control and sham + CD25-specific mAb, # p<0.05 vs. ICH + CD25-specific mAb, Mean ± SD, One-way ANOVA, Tukey test.

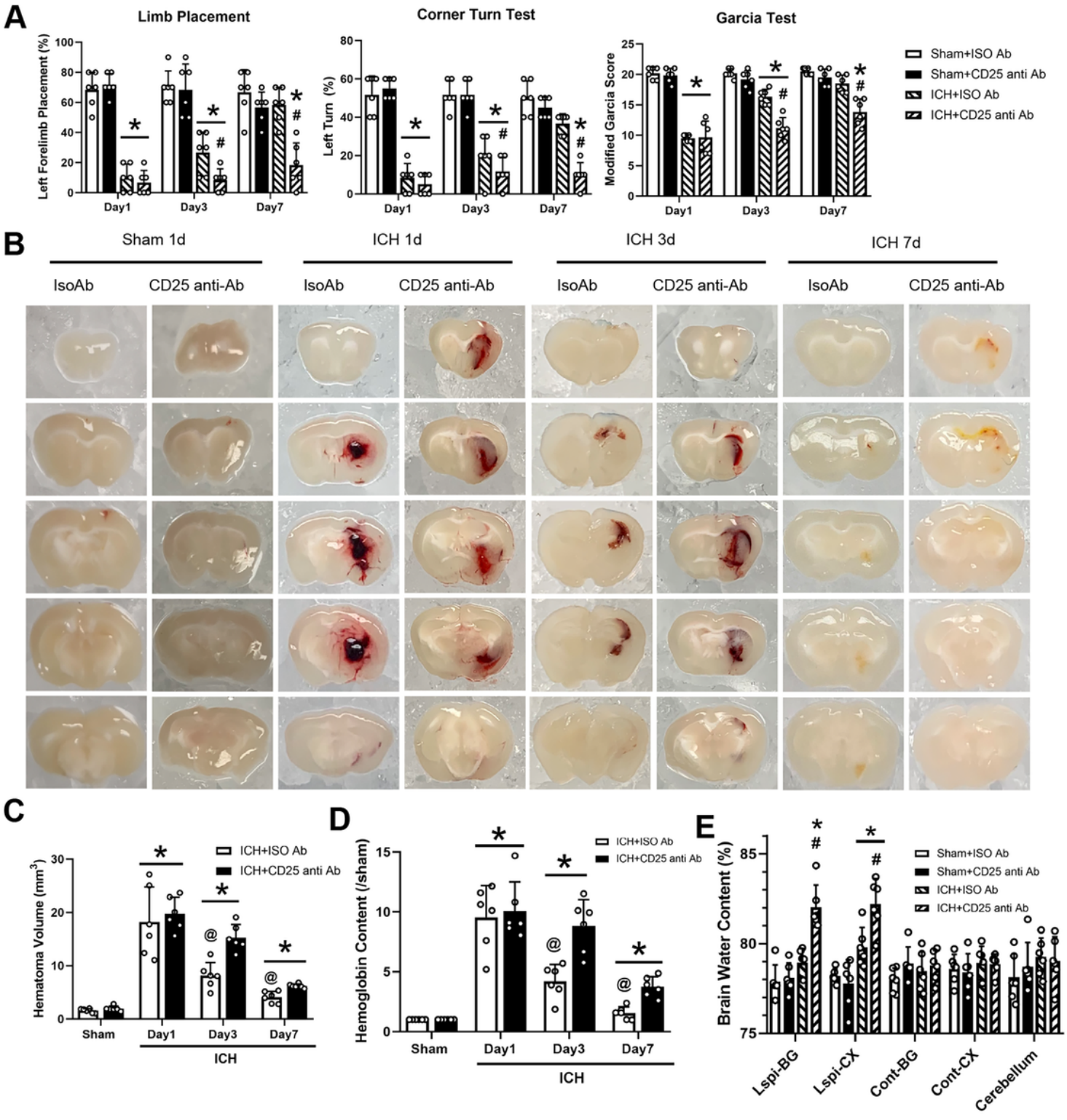

Figure 3

Tregs depletion by the CD25 antibody aggravated early brain injury after ICH. A, Short-term neurological function assessment (Modified Garcia test, Left forelimb placement test and Corner turn test) in the isotype IgG control and anti-CD25 groups at 1, 3, and 7 d after ICH. B, Representative photograph of brain sections at 1, 3, and 7 d after ICH. C, Hemoglobin content at 1, 3, and 7 d post-ICH. D, Hematoma volume at 1, 3, and 7 d post-ICH. E, Brain edema at 72 h post-ICH. n=6/group. * p<0.05 vs. sham + isotype control and sham + CD25-specific mAb, # p<0.05 vs. ICH + isotype control, @ p<0.05 vs. ICH + CD25-specific mAb, Mean ± SD, One-way ANOVA, Tukey test.

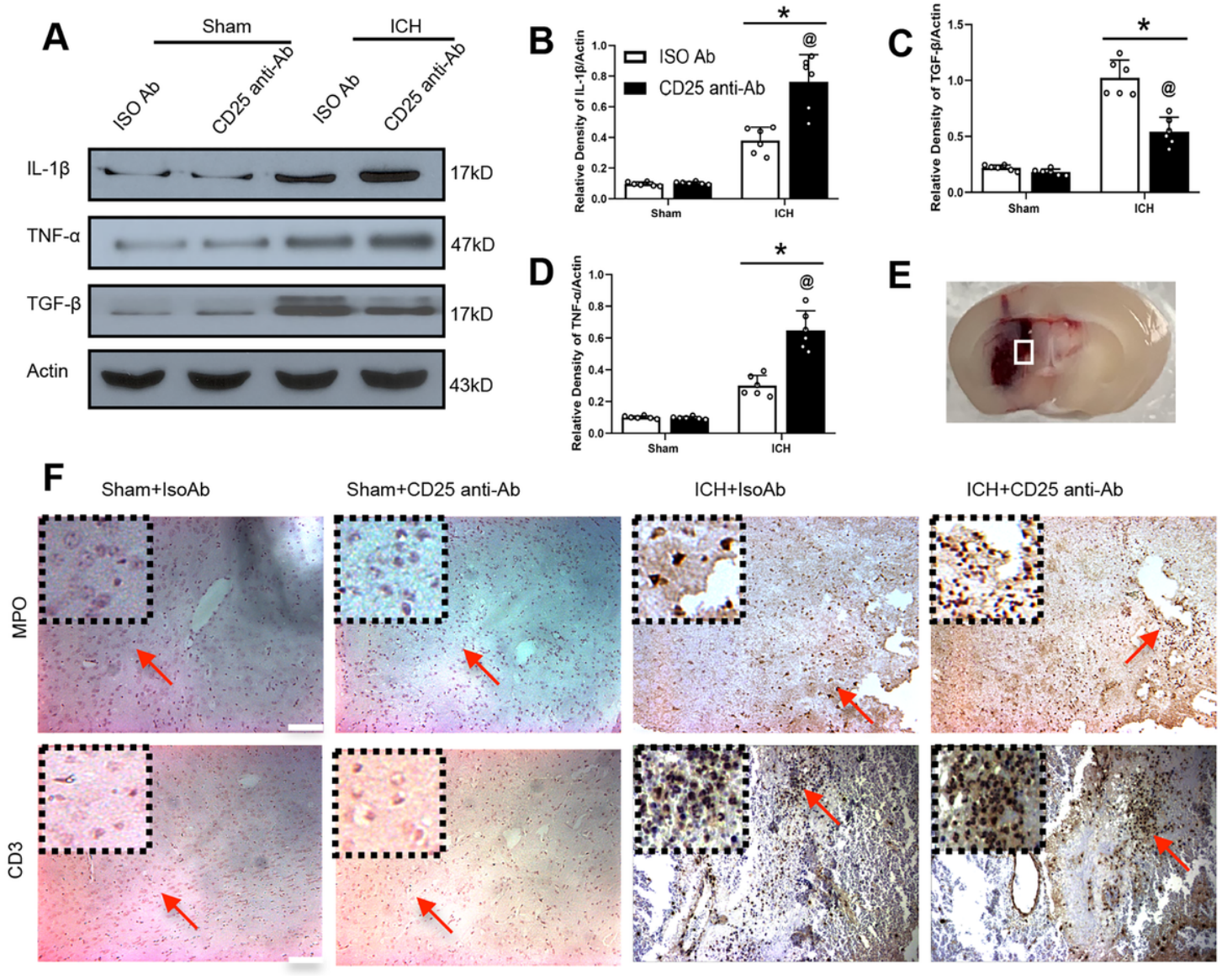

Figure 4

Tregs depletion by the CD25 antibody aggravated neuroinflammation after ICH. A-D, Representative western blot bands and quantitative analyses of IL-1β, TNF-α and TGF-β in ipsilateral brain hemisphere at 72 h after ICH. n=6/group. E-F, Representative microphotograph of immunohistochemistry staining of MPO and CD3 positive cells (yellow) in the perihematomal area at 72 h after ICH. n=4/group. * p<0.05 vs. sham + isotype control and sham + CD25-specific mAb, # p<0.05 vs. ICH + isotype control, @ p<0.05 vs. ICH + CD25-specific mAb, Mean ± SD, One-way ANOVA, Tukey test.

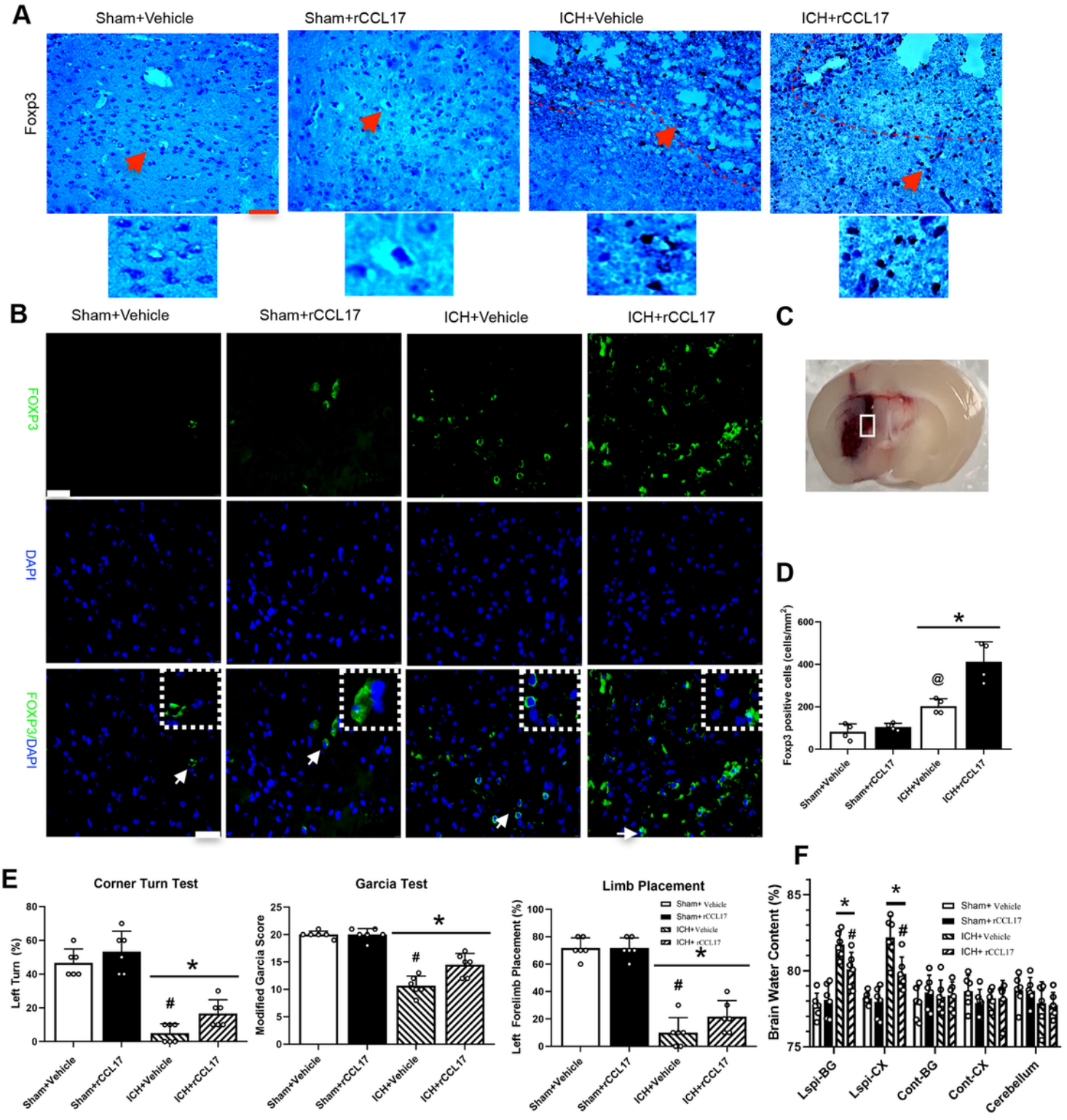

Figure 5

rCCL17-mediated Tregs recruitment alleviated the early brain injury after ICH. A, Representative microphotograph of immunohistochemistry staining of Foxp3 positive cells (brown) in the peri-hematomal area at 72 h after ICH. n=4/group. B, Brain samples with schematic illustration showing the peri-hematomal region (small white box) from where the microphotograph of immunofluorescence staining was taken. C-D, Representative microphotograph and quantitative analyses of localization of

Foxp3+ cells (green) in the peri-hematomal area at 72 h after ICH. n=4/group. E, Short-term neurological function. n=6/group. F, Brain edema at 72 h post-ICH. n=6/group, * p<0.05 vs. sham +vehicle and sham + rCCL17, # p<0.05 vs. ICH + rCCL17, @ p<0.05 vs. ICH + vehicle, Mean ± SD, One-way ANOVA, Tukey test.

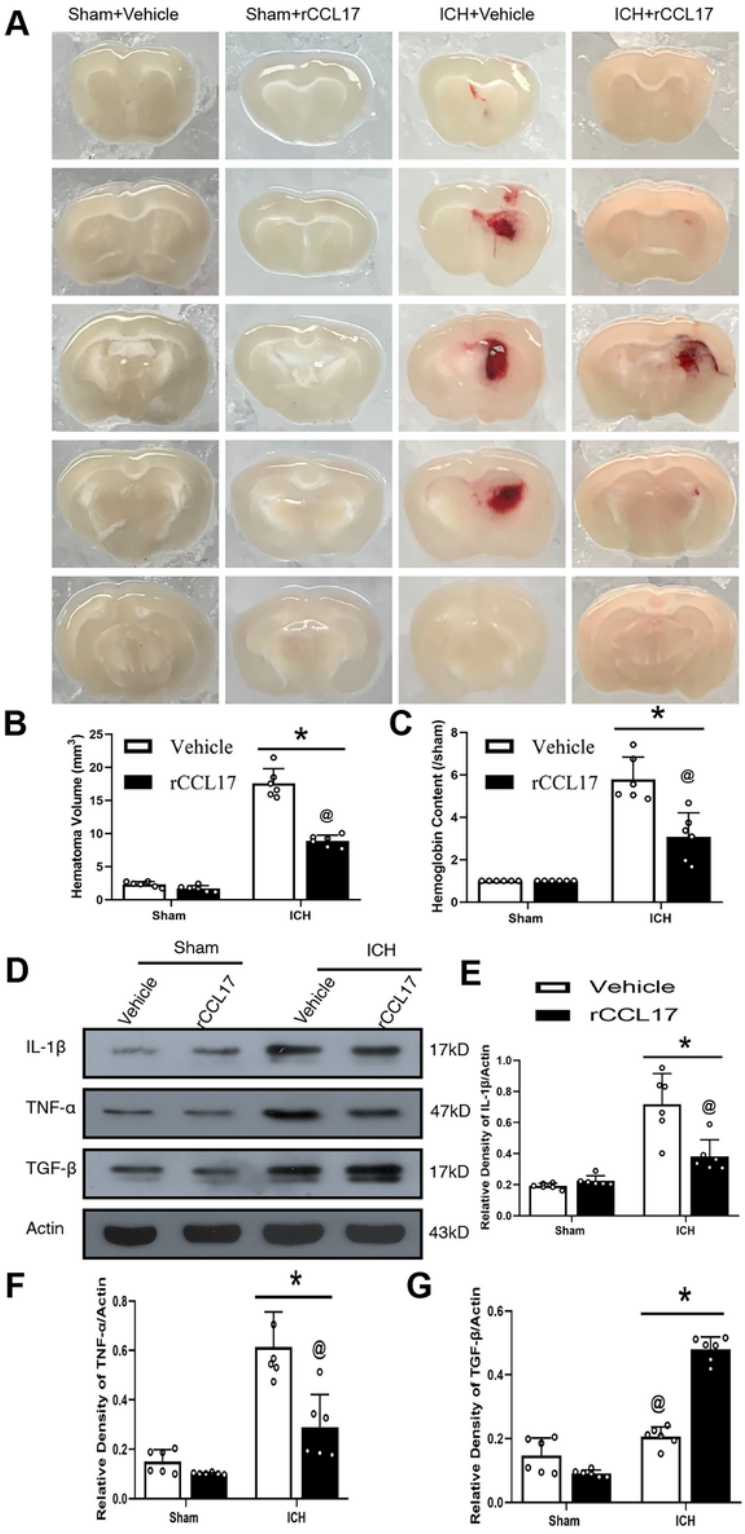

Figure 6

rCCL17-mediated Tregs recruitment alleviated hematoma and neuroinflammation after ICH. A-C, Representative photograph of brain sections, Hematoma volume, Hemoglobin content at 72 h after ICH.

D-G, Representative western blot images and quantitative analyses of IL-1β, TNF-α and TGF-β at 72 h after ICH. n=6/group. n=6/group, * p<0.05 vs. sham +vehicle and sham + rCCL17, # p<0.05 vs. ICH + rCCL17, @ p<0.05 vs. ICH + vehicle, Mean ± SD, One-way ANOVA, Tukey test.

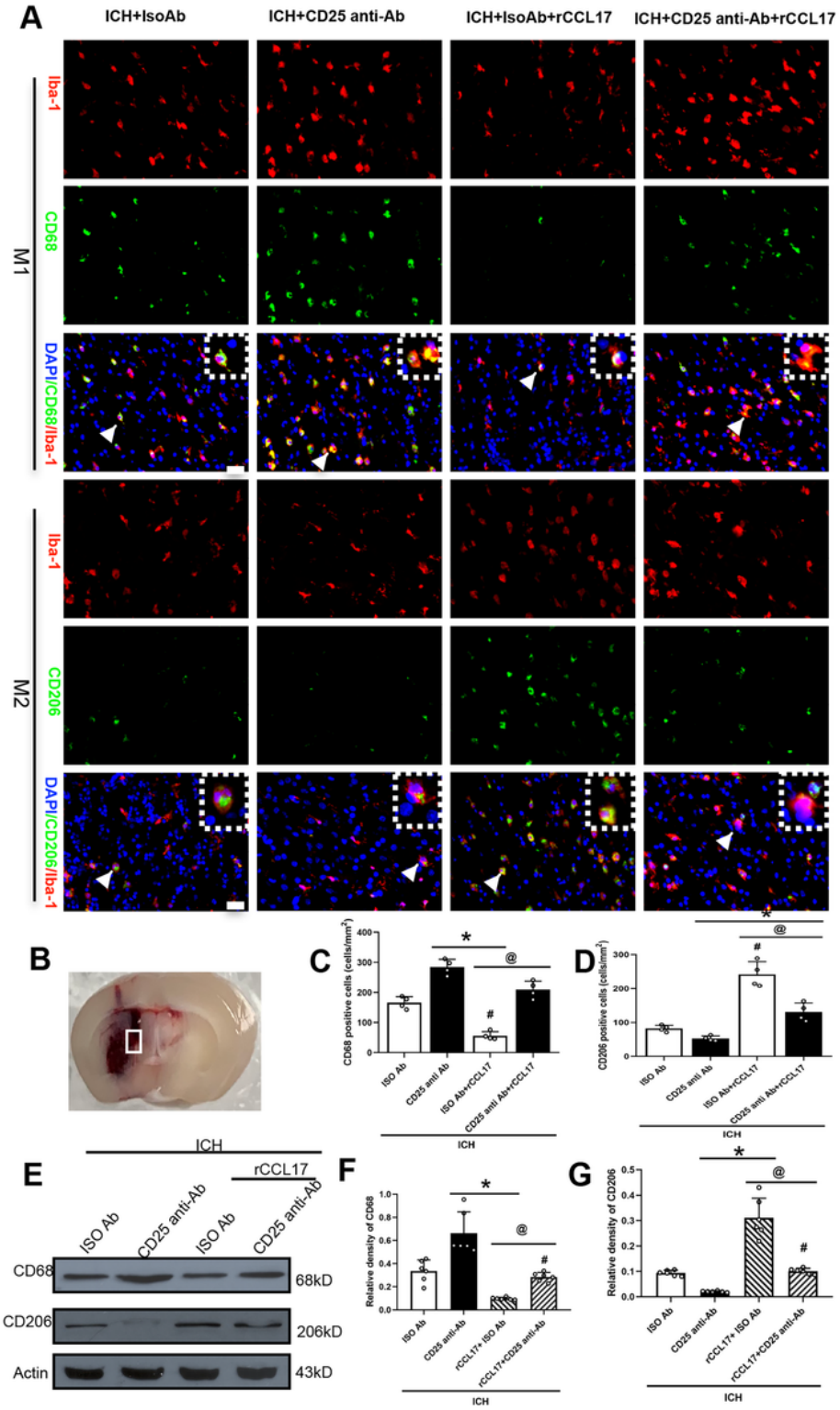

Figure 7

Tregs promoted microglial/macrophages polarization and shifted toward M2 phenotype after ICH. A-D, Representative microphotographs and quantitative analysis of co-immunofluorescence staining of CD68

(green), CD206 (green) with microglia (Iba-1, red) in the ipsilateral hemisphere at 72 h after ICH. Nuclei were stained with DAPI (blue). A small white square within coronal section of brain indicated the location from where the microphotograph of immunofluorescence staining was taken. n=4 /group. E-G, Representative western blot bands and quantitative analyses of CD68 and CD206 at 72 h after ICH. n=6/group, * p<0.05 vs. ICH + isotype control, @ p<0.05 vs. ICH + CD25-specific mAb, # p<0.05 vs. ICH + CD25-specific mAb + rCCL17, Mean ± SD, One-way ANOVA, Tukey test.

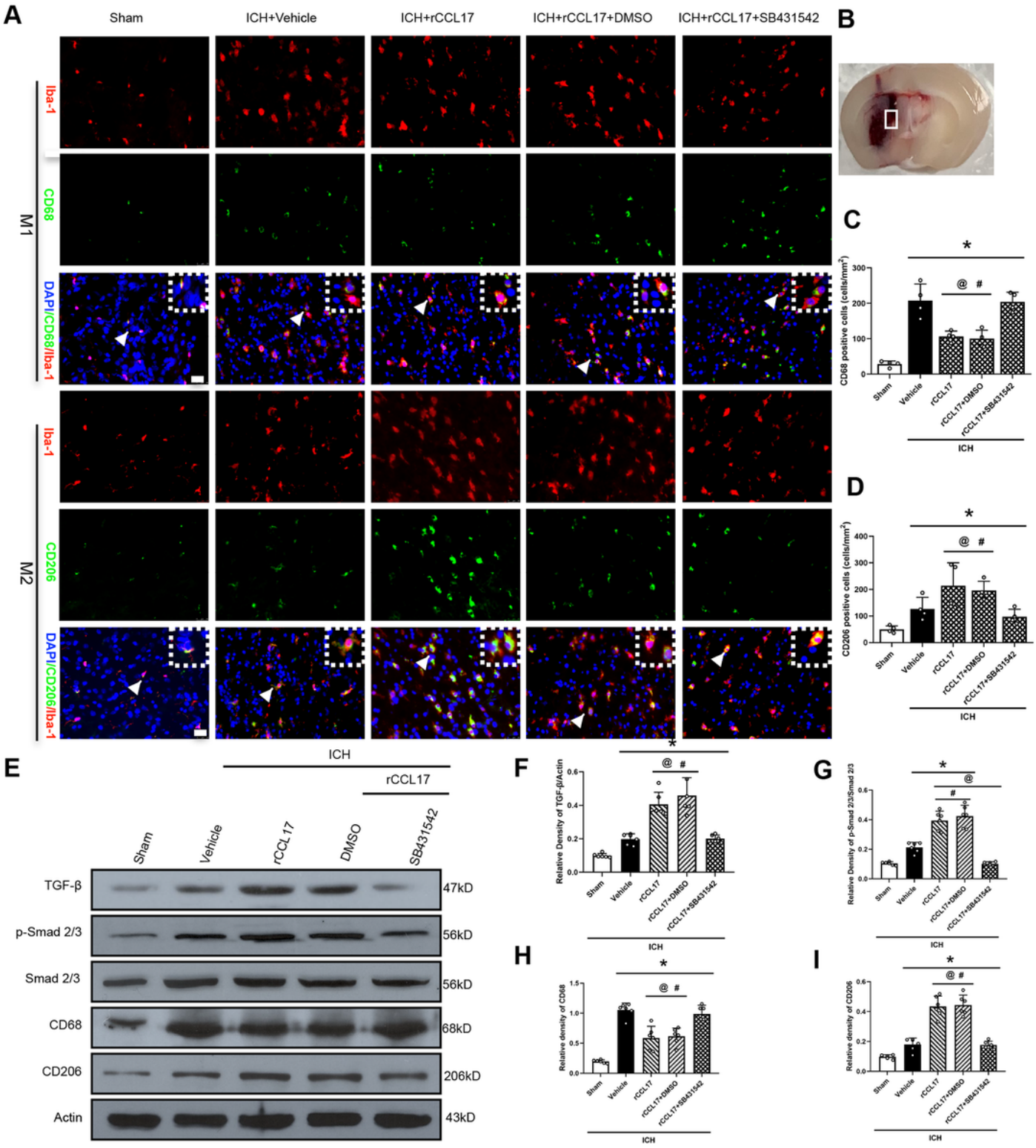

Figure 8

The TGFβ/TGFβR/Smad2/3 axis participated in Tregs-induced M2 polarization of microglia. A-D, Representative microphotographs and quantitative analysis of co-immunofluorescence staining of CD68 (green), CD206 (green) with microglia (Iba-1, red) in the ipsilateral hemisphere at 72 h after ICH. Nuclei were stained with DAPI (blue). A small white square within coronal section of brain indicated the location from where the microphotograph of immunofluorescence staining was taken. n=4 /group. E-I, Representative western blot bands and quantitative analyses of TGF-β, p-Smad2/3, CD68 and CD206 at 72 h after ICH. n=6/group, * $p<0.05$ vs. sham, @ $p<0.05$ vs. ICH + vehicle, # $p<0.05$ vs. ICH + rCCL17 + SB431542, Mean ± SD, One-way ANOVA, Tukey test.